Environ Monit Assess (2013) 185:267–277
DOI 10.1007/s10661-012-2551-y

Spatial–temporal dynamics of NDVI and Chl-*a* concentration from 1998 to 2009 in the East coastal zone of China: integrating terrestrial and oceanic components

Xiyong Hou · Mingjie Li · Meng Gao · Liangju Yu · Xiaoli Bi

Received: 30 April 2011 / Accepted: 25 January 2012 / Published online: 25 February 2012

Abstract Annual normalized difference vegetation index (NDVI) and chlorophyll-a (Chl-*a*) concentration are the most important large-scale indicators of terrestrial and oceanic ecosystem net primary productivity. In this paper, the Sea-viewing Wide Field-of-view Sensor level 3 standard mapped image annual products from 1998 to 2009 are used to study the spatial–temporal characters of terrestrial NDVI and oceanic Chl-*a* concentration on two sides of the coastline of China by using the methods of mean value (*M*), coefficient of variation (CV), the slope of unary linear regression model (Slope), and the Hurst index (*H*). In detail, we researched and analyzed the spatial–temporal dynamics, the longitudinal zonality and latitudinal zonality, the direction, intensity, and persistency of historical changes. The results showed that: (1) spatial patterns of *M* and CV between NDVI and Chl-*a* concentration from 1998 to 2009 were very different. The dynamic variation of terrestrial NDVI was much mild, while the variation of oceanic Chl-*a* concentration was relatively much larger; (2) distinct longitudinal zonality was found for Chl-*a* concentration and NDVI due to their hypersensitivity to the distance to shoreline, and strong latitudinal zonality existed for Chl-*a* concentration while terrestrial NDVI had a very weak latitudinal zonality; (3) overall, the NDVI showed a slight decreasing trend while the Chl-*a* concentration showed a significant increasing trend in the past 12 years, and both of them exhibit strong self-similarity and long-range dependence which indicates opposite future trends between land and ocean.

Keywords Spatial–temporal dynamics · Normalized difference vegetation index (NDVI) · Chlorophyll-*a* (Chl-*a*) concentration · Slope · Hurst index · East coastal zone of China

X. Hou (✉) · M. Li · M. Gao · L. Yu · X. Bi
Key Laboratory of Coastal Zone Environmental Processes, Yantai Institute of Coastal Zone Research (YIC), Chinese Academy of Sciences (CAS); Shandong Provincial Key Laboratory of Coastal Zone Environmental Processes, YICCAS, Yantai, Shandong 264003, People's Republic of China
e-mail: xyhou@yic.ac.cn

M. Li
Key Laboratory of Coastal Zone Environmental Processes, Yantai Institute of Coastal Zone Research (YIC), Chinese Academy of Sciences (CAS); Shandong Provincial Key Laboratory of Coastal Zone Environmental Processes, YICCAS; Graduate School of the Chinese Academy of Sciences, Beijing 100049, China

Introduction

Large-scale and long-term ecological studies both on land and in the sea have been one of the hotspots in multidiscipline researches under the background of global change. Both terrestrial vegetation and oceanic phytoplankton are of primary interests of NASA's Earth Observing System (EOS) program. The variation of vegetation cover not only influences the energy balance, climate, hydrological process, and the

biogeochemical cycles but also indirectly illustrates the interaction among the climate, the environment, and anthropogenic activities (Huete et al. 1999). Chlorophyll concentration, measured by the Chlorophyll-*a* (Chl-*a*) concentration, is the most fundamental variable of phytoplankton biomass and has been considered as a key index to indicate the oceanic primary productivity and the eco-environment of the sea (Campbell et al. 1995). Studies of terrestrial vegetation and Chl-*a* concentration at regional and global scales and from seasonal to decadal processes are often focused on the understanding of primary productivity, the carbon cycle, and the systematic schemes of earth functions (Campbell et al. 1995; Huete et al. 1999). However, traditional methods cannot simultaneously deal with large spatial scale and long-term time period. The advent of remote sensing technology provides the chance to monitor and reflect the large-scale distribution of terrestrial vegetation and oceanic chlorophyll as well as their biophysical and structural properties and spatial–temporal variations. Compared with the in situ measurement techniques, remote sensing data have much improved spatial–temporal coverage; consequently, remote sensing has become a powerful tool of NASA's EOS and effective means of monitoring global ecological and environmental changes (Campbell et al. 1995; Huete et al. 1999; Gobron et al. 2003). Moreover, remote sensing data have accelerated the progress of the interdisciplinary research and promoted the development of many other new disciplines.

In terrestrial area, normalized difference vegetation index (NDVI) is an important and widely used vegetation index in multidiscipline studies. Long-term spatial–temporal variations of NDVI are often used as an indicator of terrestrial ecosystem oscillation and succession. For example, Barbosa et al. (2006) analyzed the variability of NDVI over 20 years in the northeast region of Brazil; Lasaponara (2006) assessed the interannual vegetation anomalies by principal component analysis method based on the time series of NDVI data; Song and Ma (2007) studied the characteristics of vegetation cover change in Northwest China based on time series of SPOT-Vegetation data; Han et al. (2009) revealed the spatial–temporal change of vegetation in the Yangtze River Delta based on time series of remote sensing images. Variations of Chl-*a* concentration are widely used to study changes in ocean environment. Gordon and Morel (1983) and Falkowski et al. (1998) showed that the selective absorption of blue and blue green wavelengths by Chl-*a* concentration can quantify phytoplankton biomass in the contemporary oceans using satellite-derived measurements of ocean color, which provides a tool for mapping the distribution of phytoplankton biomass in the oceans and facilitates the learning of the spatial–temporal dynamics of the oceanic primary production. Continuous monitoring of spatial and seasonal patterns of near-surface phytoplankton concentrations can only realistically be achieved by ocean color remote sensing technique which can provide synoptic spatial and temporal Chl-*a* concentration data not attainable by in situ sampling (Morel and Berthon 1989; O'Reilly et al. 1998; Hyde et al. 2007). Chauhan et al. (2002) suggested that the information of the Chl-*a* concentration on a global scale is important to study the biogeochemical cycles of carbon, nitrogen, and sulfur. Later, the mesoscale variability (Uz and Yoder 2004) and the seasonal and interannual variability of Chl-*a* concentrations (Sackmann et al. 2004; Hyde et al. 2007; Krishna 2008) were studied widely.

Studies of terrestrial NDVI and oceanic Chl-*a* concentration are abundant, but these studies rarely connect the two domains together to understand the similarities and differences between changes on land and in the sea. With the accumulation of time series of remote sensing data both on land and in the sea, monitoring and studying the spatial–temporal dynamics of regional or global NDVI and Chl-*a* concentration simultaneously become possible. For example, the Sea-viewing Wide Field-of-view Sensor (SeaWiFS) on board the OrbView-2 spacecraft was specifically designed to estimate the phytoplankton pigment concentration in the oceans, but it also permits the monitoring of terrestrial land surfaces in terms of its spectral bands centered at 443 nm (blue), 670 nm (red), and 865 nm (near-infrared) (Campbell et al. 1995). In this paper, the time series of SeaWiFS products were used to calculate mean value (*M*), coefficient of variation (CV), slope of the unary linear regression model (Slope), and Hurst index (*H*) on every pixel in order to study the dynamic changes of NDVI and Chl-*a* concentration in China's east coastal zone, specifically the 300-km buffer zone on both sides of Chinese coastline (Fig. 1).

Data and methods

The SeaWiFS was launched on September 1997 by NASA to provide a long-term time series of global data products in different levels from level 0 to level 4. In this

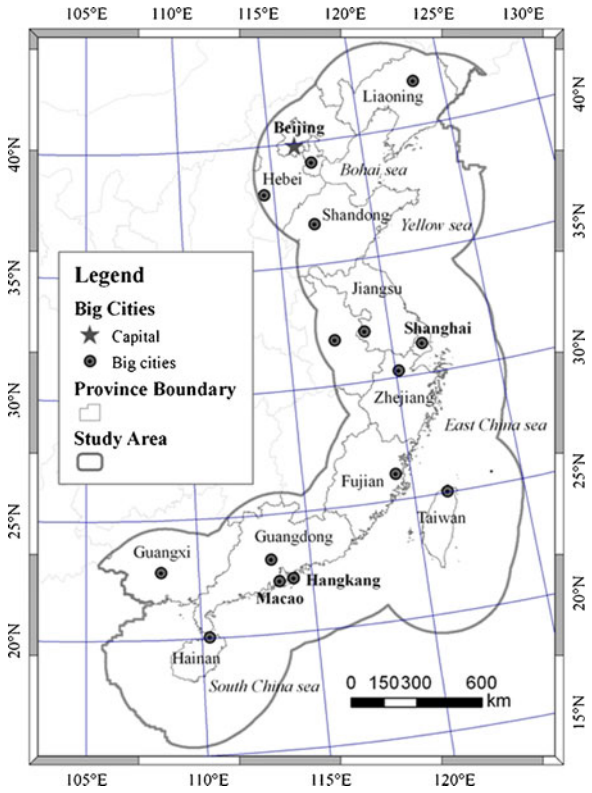

Fig. 1 Study area: China's east coastal zone which mainly covers Beijing, Tianjin, Shanghai, Hong Kong, Macao, and other ten seaside provinces on land area and Bohai Sea, Yellow Sea, East China Sea, and South China Sea in the water area. In detail, the length of coastline is 18,000 km; the extent width on both sides of the coastline is 300 km

study, the level 3 standard mapped image (SMI) annual data products of terrestrial NDVI and oceanic Chl-*a* concentration from 1998 to 2009 were used. Both the products of NDVI and Chl-*a* concentration have the same spatial resolutions of 9.28 km at the nadir of the sensor and the algorithms of the level 3 SMI annual data products are designed for macro-scale and global scale researches (Campbell et al. 1995; O'Reilly et al. 1998). The data can be obtained from the Distributed Active Archive Center under the auspices of NASA.

Dataset of terrestrial NDVI

SeaWiFS is sensitive to the wavelengths at 412, 443, 490, 510, 555, 670, 765, and 865 nm. Although the SeaWIFS sensor is originally designed for observation of ocean color, the NDVI can be calculated from the visible and near-infrared band reflectivity using band 6 at 670 nm and band 8 at 865 nm (http://oceancolor.gsfc.nasa.gov/DOCS/OCSSW/get__ndvi_8c_source.html). And the formula of NDVI can be described by the following equation:

$$\mathrm{NDVI} = \frac{B_{\mathrm{IR}} - B_{\mathrm{R}}}{B_{\mathrm{IR}} + B_{\mathrm{R}}} \tag{1}$$

where B_{IR} and B_{R} are the near-infrared band and red band reflectance, respectively.

The global annual NDVI products are provided by the SeaWiFS Project at Goddard Space Flight Center. The level 3 SMI annual data products of NDVI from 1998 to 2009 are encoded as HDF4 raster format data with the pixel digital number value from 0 to 65,535. It is necessary to retrieve the actual NDVI value by a series of transformation using Eq. 2.

$$\mathrm{NDVI_f} = \mathrm{DN} \times 1.47828e^{-5} - 0.05 \tag{2}$$

where $\mathrm{NDVI_f}$ is the actual value of NDVI, and DN is the digital number of the level 3 NDVI products.

Dataset of oceanic Chl-*a* concentration

The global annual Chl-*a* concentration level 3 SMI data products from 1998 to 2009 were used. The current algorithm of SeaWiFS Chl-*a* concentration is the ocean chlorophyll 4 (OC4) algorithms (O'Reilly et al. 1998). And the evaluation of SeaWiFS chlorophyll-*a* product suggested that regional algorithms do not significantly improve the global algorithm estimates, and the OC4 algorithm showed the best performance among all the algorithms examined (Dogliotti et al. 2009). OC4 is a modified cubic polynomial relating the ratio of the reflectance in the blue (wavelength at 443, 490, or 510 nm) and green (wavelength at 555 nm) bands to the Chl-*a* concentration.

$$\mathrm{Chla} = 10.0^{(0.366 - 3.067R_{\max} + 1.930R^2{}_{\max} + 0.649R^3{}_{\max} - 1.532R^4{}_{\max})} \tag{3}$$

where Chla is the Chl-*a* concentration and $R_{\max}$ is the maximum band ratio from the remote sensing reflectance (R_{rs}) ratios at the given wavelengths. The $R_{\max}$ can be obtained with the following equation:

$$R_{\max} = \log_{10}\left(\frac{R_{\mathrm{rs}}443}{R_{\mathrm{rs}}555}\right\rangle \frac{R_{\mathrm{rs}}490}{R_{\mathrm{rs}}555}\left\rangle \frac{R_{\mathrm{rs}}510}{R_{\mathrm{rs}}555}\right) \tag{4}$$

where R_{rs} is the ratio of leaving water irradiance to the down-welling surface irradiance and the Eqs. 3 and 4

describe the polynomial best fit that relates log-transformed Chl-*a* concentration to a log-transformed ratio of remote sensing reflectance.

Mean value and coefficient of variation

The mean value (M) of annual NDVI and Chl-*a* concentration data sequence from 1998 to 2009 on every pixel is a basic indicator to represent the temporal central tendency, and CV of these data sequence on every pixel is a basic indicator to depict the temporal discrete degree. Both of them are very useful statistical indices. In this study, M and CV of the time series remote sensing data of NDVI and Chl-*a* concentration were calculated on the pixel scale in order to find their basic statistical characteristics.

Slope of unary linear regression model

In order to depict the temporal trends concisely, the unary linear regression model (ULRM) was used to calculate the slope of time series of remote sensing data based on the pixel values from 1998 to 2009 (Song and Ma 2007; Han et al. 2008). Slope can avoid the bias of the range analysis method caused by occasional factors of both the starting and the ending year. The formula of ULRM is as follows:

$$\mathrm{NDVI}(\mathrm{Chl}-a) = \mathrm{Slope} \times \tau + c \tag{5}$$

where τ is the temporal range, it ranges from 1 to 12 because the temporal range in this paper is 12 years, and c is the intercept of a line. The annual NDVI and Chl-*a* concentration is assumed as linear function of temporal variable, and the Slope is what we want to get from time series NDVI and Chl-*a* concentration data using Eq. 6.

$$\mathrm{Slope} = \frac{n \times \sum_{i=1}^{n} i \times \mathrm{NDVI}_i(\mathrm{Chla}_i) - \sum_{i=1}^{n} i \sum_{i=1}^{n} \mathrm{NDVI}_i(\mathrm{Chla}_i)}{n \times \sum_{i=1}^{n} i^2 - \left(\sum_{i=1}^{n} i\right)^2} \tag{6}$$

where n is the temporal range, the same as the τ in Eq. 5; NDVI_i (Chla_i) is the value of NDVI (or Chl-*a* concentration) in the year i, and the Slope obtained by ULRM can quantitatively depict the historical trend of NDVI (or Chl-*a* concentration). In detail, Slope>0 means that the increased tendency of NDVI (or Chl-*a* concentration) while Slope<0 means that the decreased tendency of NDVI (or Chl-*a* concentration).

Hurst index

Hurst index (H) is one of the most effective methods to depict the self-similarity and long-range dependence for the time series data. And the rescaled range analysis (R/S) method is one of the most common methods to calculate the Hurst index (Rao and Bhattachary 1999; Han and Tang 2004); the basic principles are as follows: for a time series, τ is the temporal range and $R_{(\tau)}$ and $S_{(\tau)}$ are the range deviation sequence and the standard deviation sequence, respectively, c is a constant number, and H is the Hurst index. There is an exponential equation as follows:

$$\frac{R(\tau)}{S(\tau)} = (c, \tau)^H \tag{7}$$

Using Eq. 7, H can be calculated based on the observed time series of remote sensing data. If H=0.5, the time series shows an independent random process; if H>0.5, the time series is a persistent series, in other words, if there is a positive increment in the average sense in the past, there will be a increase in the future; if H<0.5, the time series suggests an anti-persistent series, that is, a decreasing trend in the past will change into an increasing trend in the future.

Flow chart of data processing and methodology

As mentioned above, the mean value, the CV, the Slope, and the Hurst index were used to analyze the spatial–temporal characters of the NDVI and the Chl-*a* concentration. In Fig. 2, a flow chart of data processing, methodology, and analysis of corresponding results was illustrated.

Results

Statistical characteristics of time series of NDVI and Chl-*a* concentration

Spatial patterns of M_{NDVI} and M_{Chla} from 1998 to 2009 were very different (Fig. 3). In the terrestrial

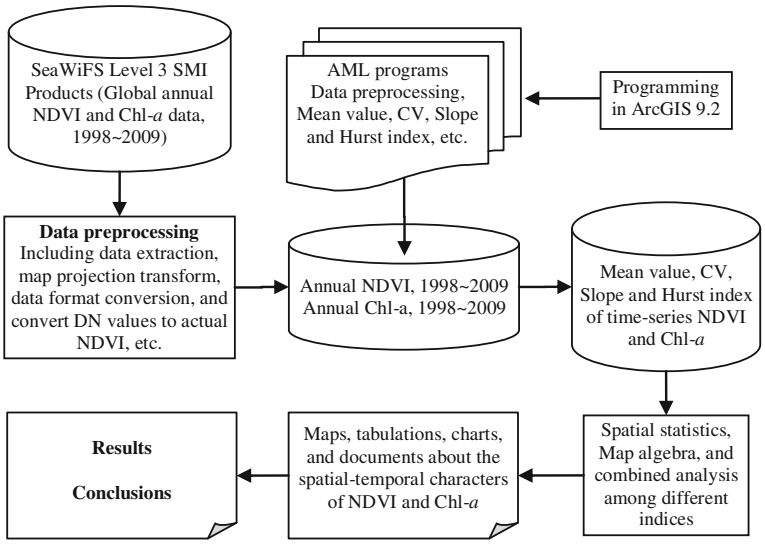

Fig. 2 Flow chart of the NDVI and Chl-*a* concentration data processing based on SeaWiFS level 3 SMI products and ARC Macro Language in ArcGIS 9.2 software

area, high NDVI values were mainly in the southeast and northeast of the study area (south of 30° N and north of 40° N) where there were semitropical and temperate forests, respectively. In the oceanic area, high Chl-*a* concentration values were found mainly between 30° N and 40° N where there were long silty beaches and big estuaries include Yangtze River estuary, Yellow River estuary, Liao River estuary, and so on.

In terrestrial areas, the *M* and the CV of NDVI showed a distinct opposite numerical relationships that the higher *M* corresponded to lower CV, while the lower *M* corresponded to higher CV simultaneously (Figs. 4 and 5) which indicate that the annual NDVI was very steady. However, in most areas of the ocean, the numerical relationships between *M* and CV of Chl-*a* concentration were much disorganized (Figs. 4 and 5), especially in areas nearby the Yangtze River estuary and the northern coastal area of Zhejiang Province, there were higher *M* and higher CV of Chl-*a* concentration simultaneously which indicated that the annual Chl-*a* concentration fluctuate acutely. The visible difference of *M* and CV relationships indicated that from 1998 to 2009, the temporal variation of NDVI was mild, while that of Chl-*a* concentration was notable.

Zonality characters

Zonality is one of the most important geospatial patterns of many geographical phenomena from regional scale to global scale. Commonly, it includes longitudinal zonality and latitudinal zonality. The longitudinal zonality refers to the spatial patterns which are dominated by the gradient features of moisture mainly between sea and land; while the latitudinal zonality refers to the spatial patterns which are dominated by the gradient

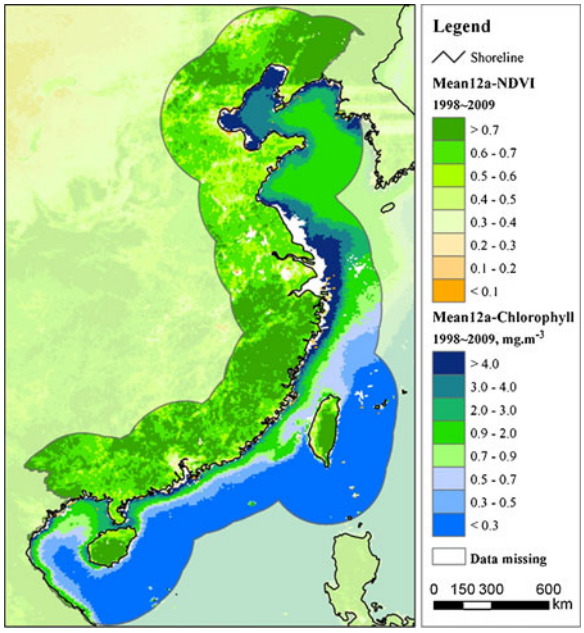

Fig. 3 Mean value of NDVI and Chl-*a* concentration. In detail, the *M* of the NDVI is a dimensionless variable, while the *M* of the Chl-*a* concentration is one variable that has concentration dimension. However, the difference will not disturb the comparability between them and very different spatial patterns can be found clearly. Furthermore, the color setting in the study area is absolute transparent effects while its semitransparent effects out of the study area. The same settings were used in maps in Figs. 4, 8, and 9 in order to keep visual continuity

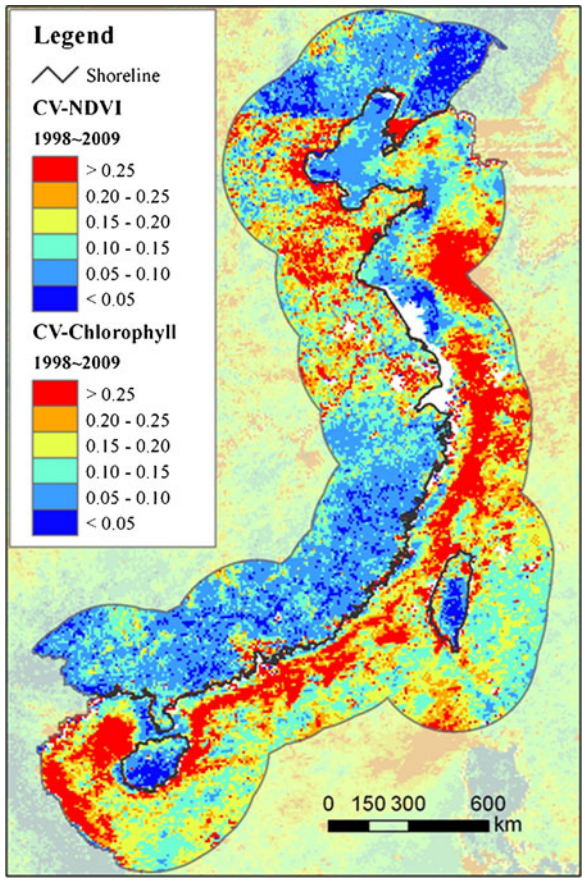

Fig. 4 CV of NDVI and Chl-*a* concentration. CV is a dimensionless variable, and therefore, the same grade thresholds in the legend were adopted in order to assure the comparability between land and ocean. The map indicates that annual Chl-*a* concentration fluctuates acutely in most areas in the sea, while the annual NDVI fluctuates very mildly in most areas of the land

features of temperature mainly along the meridian direction. We divided the whole study area into twelve 50-km-wide buffer zones on both sides of the coastline in order to detect the longitudinal zonality of NDVI and Chl-*a* concentration. The mean value (*M*) of annual NDVI and Chl-*a* concentration in 12 buffer zones from 1998 to 2009 was summarized by the zonal analyst commands in ArcGIS9.2 (Fig. 6). Obviously, it was very different between the NDVI and Chl-*a* concentration. The NDVI showed the parabolic trend, in detail, the "peak" value was located within the zone of 100~150 km away from the shoreline, and on both sides of this zone, it decreased gradually. However, the Chl-*a* concentration showed an obvious negative linear trend, in other words, the nearer the buffer zones to the shoreline, the higher the Chl-*a* concentration. Similar method was used to detect the latitudinal zonality of the mean value (*M*) of annual NDVI and Chl-*a* concentration (Fig. 7). The whole study area locates between 18.2° N and 43.6° N on land and 15.3° N and 40.9° N in the sea. The *M* of NDVI and Chl-*a* concentration per two latitudes were summarized. Obviously, except for the region that locates between 30° N and 34° N, the Chl-*a* concentration showed an obviously increasing trend along with the increasing of the latitudes. However, the NDVI showed a fluctuant and ruleless trend along with the increasing of the latitudes.

Spatial patterns of Slope and Hurst index

The Slope and the Hurst index (*H*) of the time series of SeaWiFS products from 1998 to 2009, respectively, showed the dynamic tendency of NDVI and Chl-*a* concentration in the past 12 years and their long-range dependence which can indicate the anticipatory sustainability of their previous dynamic tendency (Figs. 8 and 9). As shown in Fig. 8, the Slope of the Chl-*a* concentration in the sea varies from −0.47 to 1.09, whereas the Slope of the NDVI on the land varies from −0.07 to 0.06; the range in the sea was more than 1.56, while it was less than 0.13 on the land. The ratio of the range in the sea to that on the land reached up to 12. The distinct difference indicated that, overall, the temporal fluctuation of Chl-*a* concentration was very large while it was much small for the NDVI. However, on the land, the amounts of pixel that had the negative Slope accounted for 69% and the mean value of all the pixels was −0.0058, which indicated that, overall, the vegetation on the land degenerated remarkably in the past 12 years. On the contrary, in the sea, the amounts of pixel that had the negative Slope accounted for 24% only and the mean value of all the pixels was 0.0114, which indicated that, overall, the Chl-*a* concentration in the sea improved greatly in the past 12 years. Spatial patterns of Slope both on the land and in the sea were very complex. On the land, remarkably, a wide range of vegetation degeneration could be found such as the three metropolitan areas (Beijing–Tianjin–Tangshan Area, Yangtze River Delta, and Pearl River Delta), the southeast and west of Shandong Province, most parts of Jiangsu Province and Zhejiang Province, and so on. Areas where the vegetation improved distinctly include Liaoning Province, the north and south of Hebei Province, Shandong Peninsula, Guangxi Province and

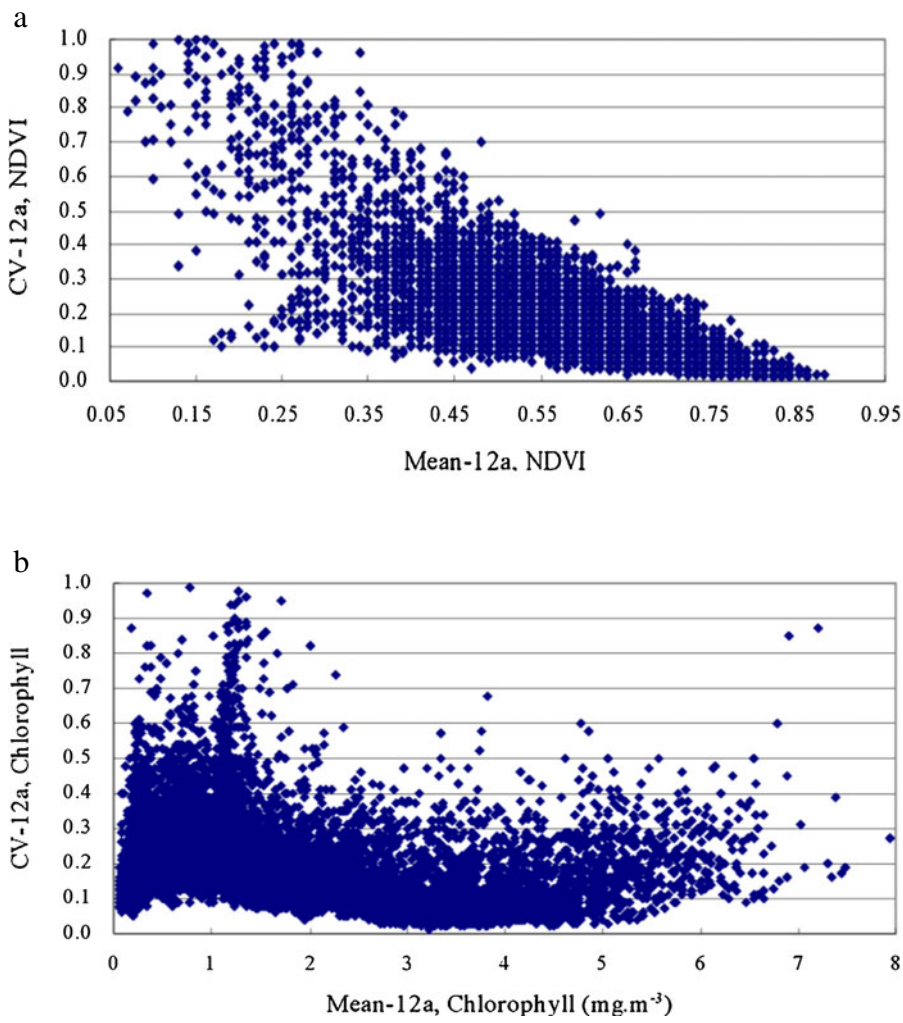

Fig. 5 Numerical relationships between *M* and CV (**a**) of annual NDVI and Chl-*a* (**b**) concentration. Each point is one pixel in the maps of Figs. 3 and 4. **a** In detail, on the land, most pixels have *M* of NDVI great than 0.35 and CV of NDVI less than 0.6, and the bigger the *M*, the smaller the CV. **b** In the sea, most pixels have *M* of Chl-*a* concentration less than 6 mg m^{-3} and CV of Chl-*a* concentration less than 0.4 and lots of pixels have lower *M* and lower CV simultaneously

Hainan Province, and so on. In the sea, significantly, a wide range of increasing phytoplankton could be found such as most parts of the Bohai Sea and the Yellow Sea, the Taiwan Strait, the coastal area of Fujian and Guangdong Provinces, the North Bay Gulf, and so on. At the same time, areas include the north and west of the Bohai Sea, the coastal area of Jiangsu Province and Guangdong Province; the mid-west of the East China Sea showed obvious decreasing phytoplankton.

As shown in Fig. 9, *H* was used to depict the self-similarity and long-range dependence of the time series SeaWiFS products. The regional mean value of *H* for NDVI and Chl-*a* concentration were 0.6869 and 0.6895, respectively, which indicated that, overall, both NDVI

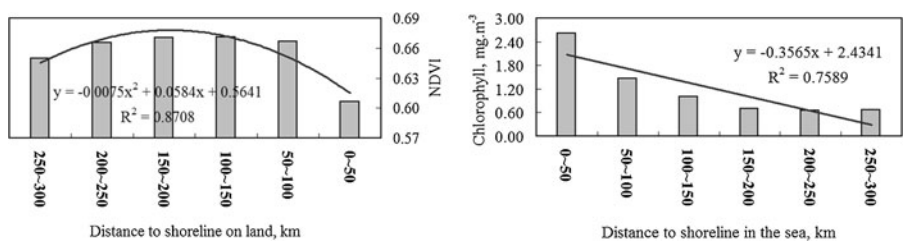

Fig. 6 The mean value (*M*) of annual NDVI and Chl-*a* concentration in twelve 50-km-wide buffer zones from 1998 to 2009 which shows the longitudinal zonality

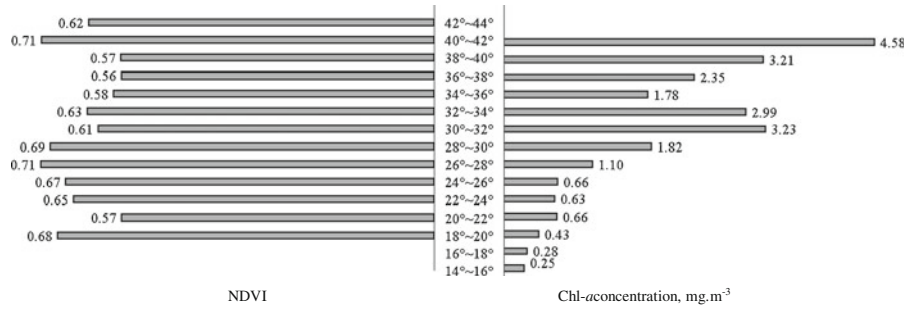

Fig. 7 The mean value (*M*) of NDVI and Chl-*a* concentration per two latitudes from 1998 to 2009 which shows the latitudinal zonality

and Chl-*a* concentration had a positive long-range dependence. However, the spatial patterns of *H* between NDVI and Chl-*a* concentration were very different. A spatial discontinuousness and unwanted salt-and-pepper noise were very prominent on the land. However, a spatial agglomeration and continuity in many parts of the sea were very obvious. In detail, the distinctly agglomerated areas include the middle and south of the Bohai Sea, the mid-west and south of the Yellow Sea, the coastal area of southern Guangdong Province, the North Bay, and so on.

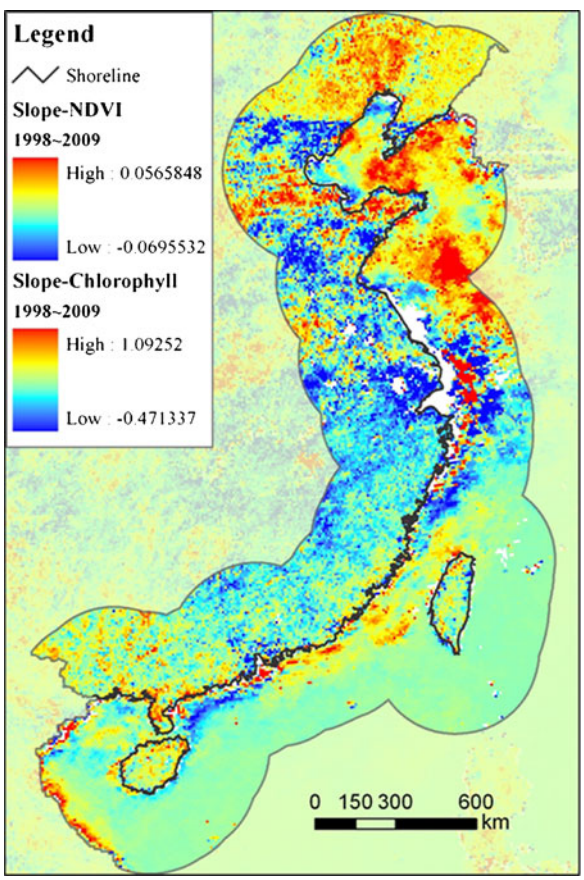

Fig. 8 Slope of the time series of SeaWiFS products from 1998 to 2009 shows the dynamic tendency of NDVI and Chl-*a* concentration in the past 12 years

Scatter plots between Slope and "*H* minus 0.5" were created for NDVI and Chl-*a* concentration, respectively, on pixel scale in order to vividly reveal the sequential dynamic characters by linking the past and the future. Different combination patterns between the Slope and *H* indicate different ecological evolvement characters. As shown in Fig. 10, each point on the scatter plots is one pixel in the spatial data of NDVI or Chl-*a* concentration. There are four quadrants in the Cartesian coordinate system which depict four kinds of Slope-($H-0.5$) combination patterns. Pixels fall into the first quadrant correspond to spatial areas that the NDVI or Chl-*a* concentration improved overall in the past and this improving trend will most possibly persist in the near future. Pixels fall into the second quadrant correspond to spatial areas that the NDVI or Chl-*a* concentration decreased overall in the past and this decreasing trend will most possibly persist in the near future, and this pattern is the alert for the ecological crisis. Obviously, not only on the land but also in the sea, most pixels fall into these two quadrants and a few pixels fall into the third or the fourth quadrant. And furthermore, the marked difference between NDVI and Chl-*a* concentration is the ratios of pixels fall into the first quadrant to that fall into the second quadrant. The results of the combination between Slope and *H* showed that the amounts of pixels fell into the first quadrant were 5,341 and 13,972 for NDVI and Chl-*a* concentration, respectively, which accounted for 26.36% and 71.40% to the land area and sea area, respectively. And the amounts of pixels fell into the second quadrant were 14,844 and 5,544 for NDVI and Chl-*a* concentration, respectively, which accounted for 73.52% and 28.33% to the land area and sea area, respectively.

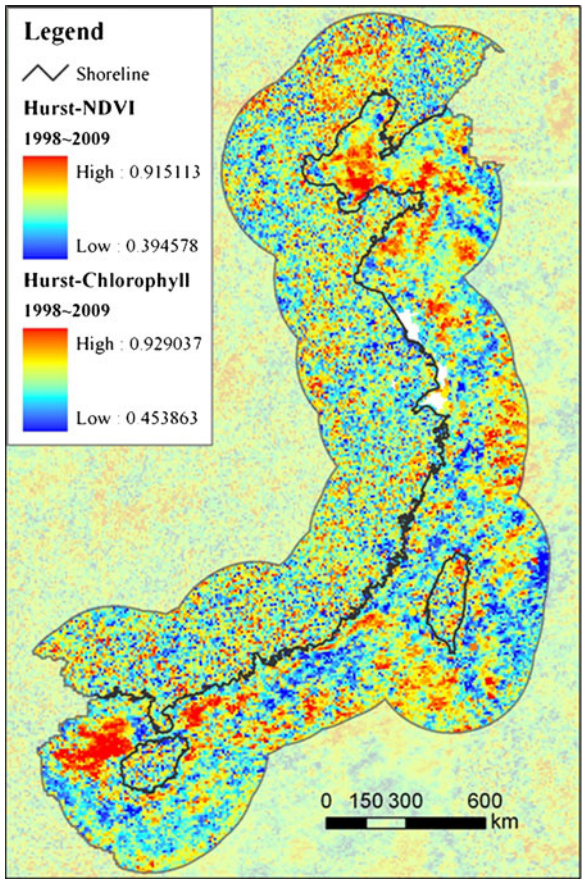

Fig. 9 Hurst index (*H*) of the time series of SeaWiFS products from 1998 to 2009 shows long-range dependence which indicates the anticipatory sustainability of previous dynamic tendency

Discussion and conclusions

Both the terrestrial NDVI and oceanic Chl-*a* concentration data were provided by the SeaWiFS project and their spatial resolution and temporal extent were completely coincident. Therefore, the annual NDVI and Chl-*a* concentration from 1998 to 2009 were used to study the overall ecological evolvement tendencies on both sides of Chinese coastline. Despite of the insufficiency of low spatial resolution, the coarse spatial–temporal resolution could not only reduce the demand for computing abilities but also mitigate the influence of numerous local and stochastic extreme events caused by environmental factors, climate factors, and human activities on small spatial scales. And therefore, from the perspective of long-term ecological evolvement dynamics on macro spatial scale, time series spatial data of SeaWiFS NDVI and Chl-*a* concentration contain more confidential, more valuable, and more explicit information than that embodied in remote sensing data sets that have much fine resolutions.

On the other hand, more and more kinds and amounts of remote sensing data have posed great challenges on methodologies and techniques of spatial–temporal data mining. In this paper, several simple but effective methodologies, such as *M*, CV, Slope, *H*, were used to reveal the dynamics of NDVI and Chl-*a* concentration on both sides of Chinese coastline. In detail, the combination of *M* and CV shows the quantity feature and temporal fluctuation characters, and the combination of Slope and *H* reveals the ecological evolvement characters by linking the past and the future. The results have proved their effectiveness in long-term and large-scale ecological information detection based on time series of remote sensing dataset. Specifically, the overall spatial–temporal dynamics of NDVI and Chl-*a* concentration from 1998 to 2009 on both sides of Chinese coastline are as follows:

1. The *M* and CV calculated on the pixel scale of time series NDVI and Chl-*a* concentration data from 1998 to 2009 indicate that their spatial patterns are very different from each other, and the temporal fluctuation of Chl-*a* concentration was very significant, whereas NDVI was very weak.
2. Both NDVI and Chl-*a* concentration are spatially hypersensitive to the distance to shoreline, and distinct parabolic character can be found for buffer-zonal values of NDVI, whereas negative linear character can be found for buffer-zonal values of Chl-*a* concentration. The difference indicates that Chl-*a* concentration has much stronger longitudinal zonality than NDVI. Similarly, the Chl-*a* concentration has much stronger latitudinal zonality than NDVI.
3. The range of Slope in the sea was much wider than that on the land which indicates that annual Chl-*a* concentration is more changeable and more unstable than annual NDVI; the obvious spatial difference of *H* between the land and the sea indicates that very locally controlling factors dominate the spatial patterns of NDVI's long-range dependence while controlling factors over a large scale dominate the spatial patterns of phytoplankton's long-range dependence.
4. The combination of Slope and Hurst index reveals a sharp contrast and very reverse ecological evolvement characters between land and sea alongside the

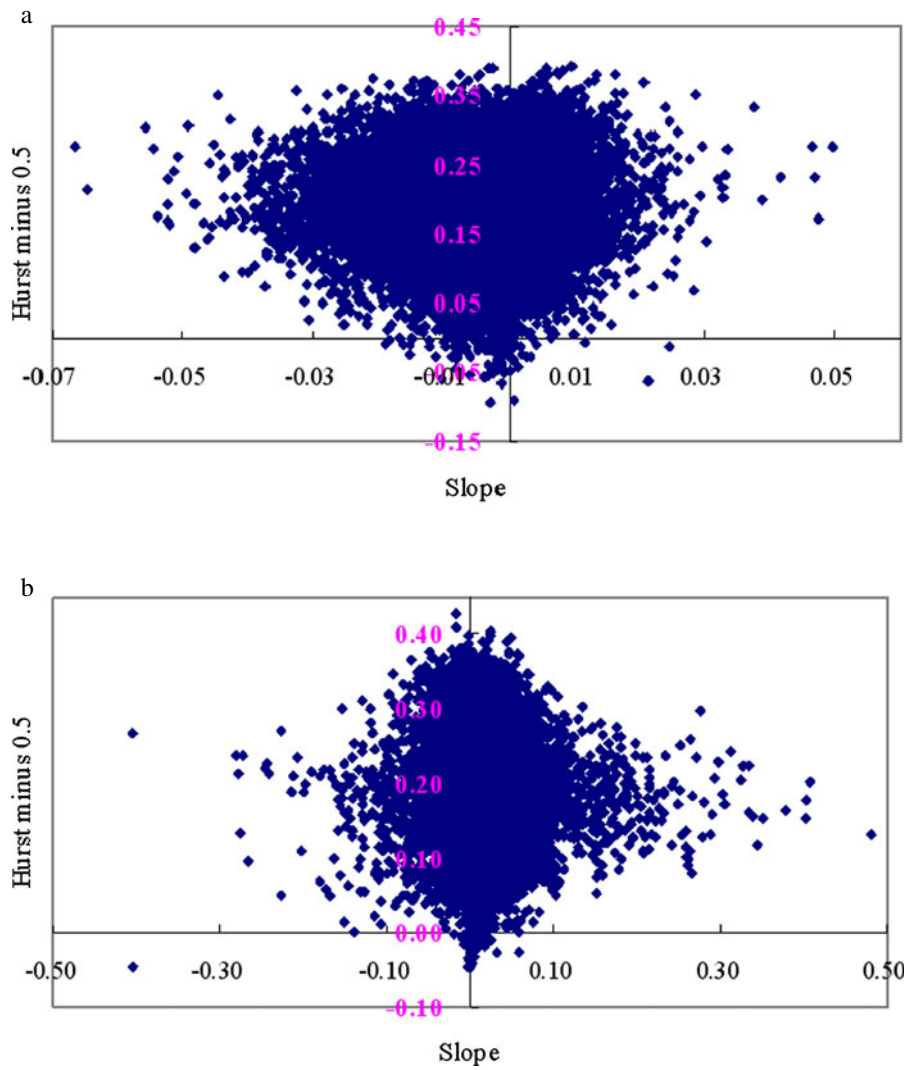

Fig. 10 Scatter plots between Slope and "*H* minus 0.5" were created for NDVI (**a**) and Chl-*a* (**b**) concentration, respectively, on pixel scale in order to vividly reveal the sequential dynamic characters by linking the past and the future. **a** Co-relationships between the Slope and Hurst index of the time series of NDVI. **b** Co-relationships between Slope and Hurst index of the time series of Chl-*a* concentration

Chinese coastline. In specific, there is nearly opposite ecological evolvement dynamics between NDVI on the land and Chl-*a* concentration in the sea. A majority of areas on the land had been and are going to encounter visible ecological degradation, whereas a majority of areas in the sea had been and are going to show visible increasing tendencies of phytoplankton continually.

The findings in this paper give us a clue of multi-angle observation and monitoring of long-term ecological variations on the land and in the sea simultaneously using time series of satellite imagery by data mining techniques. With regard to issues closely related to findings in this study, such as the reasons of the dynamics of NDVI and Chl-*a* concentration and the reasons of the differences between them, substantial evidence reported in many academic articles (Song and Ma 2007; Han et al. 2009; Sun et al. 2011; Kim et al. 2009; Hong et al. 2011; Karakaya and Evrendilek 2011) prove that human activities, especially rapid urban sprawl, exploitation of natural resources, and extensive land use changes, are most probably the main driving forces of NDVI variations on decadal time scale, although climate changes, such as variations of temperature and precipitation have great impacts on it also, and variations of sea surface temperature, suspended sediment concentration, nutrient inputs from land, and lots of land-based human activities have great impacts on spatial–temporal dynamics of Chl-*a* concentration directly or indirectly. Of course, there are more complicated driving forces and more

specific processes on local scale that significantly affect the dynamics of NDVI or Chl-*a* concentration within such a vast spatial area in this study, which are meaningful issues worthy of more research in the future.

Acknowledgments The authors acknowledge a number of individuals, groups, and organizations for their excellent works on SeaWiFS sensor designing and launching and the NDVI and chlorophyll product processing and sharing. We would like to thank Prof. Ping Shi, Dr. Song Qian, Prof. Dongyan Liu, and Dr. Dejuan Jiang for their pertinent amendments on the manuscript. The research was founded by the Knowledge Innovation Program of the Chinese Academy of Sciences (kzcx2-yw-224), the CAS Strategic Priority Research Program (XDA05130703). And, the authors gratefully acknowledge the support of K.C. Wong Education Foundation, Hong Kong.

References

Barbosa, H. A., Huete, A. R., & Baethgen, W. E. (2006). A 20-year study of NDVI variability over the northeast region of Brazil. *Journal of Arid Environments, 67*, 288–307.

Campbell, J. W., Bleisdell, J. M., & Darzi, M. (1995). Level-3 SeaWiFS data products: Spatial and temporal binning algorithms. NASA Tech. Memo. 104566, Vol. 32, S.B. Hooker, E. R. Firestone, & J.G. Acker, NASA Goddard Space Flight Center, Greenbelt, Maryland, 73. http://oceancolor.gsfc.nasa.gov/SeaWiFS/TECH_REPORTS/PreLPDF/PreLVol32.pdf

Chauhan, P., Mohan, M., Sarngi, R. K., Kumari, B., Nayak, S., & Matondkar, S. G. P. (2002). Surface chlorophyll a estimation in the Arabian Sea using IRS-P4 Ocean Colour Monitor (OCM) satellite data. *International Journal of Remote Sensing, 23*, 1663–1676.

Dogliotti, A. I., Schloss, I. R., Almandoz, G. O., & Gagliardini, D. A. (2009). Evaluation of SeaWiFS and MODIS chlorophyll-*a* products in the Argentinean Patagonian Continental Shelf (38° S–55° S). *International Journal of Remote Sensing, 30*, 251–273.

Falkowski, P. G., Barber, R. T., & Smetacek, V. (1998). Biogeochemical controls and feedbacks on ocean primary production. *Science, 281*, 200–206.

Gobron, N., Mélin, F., Pinty, B., Verstraete, M. M., Widlowski, J. L., & Bucini, G. (2003). A global vegetation index for SeaWiFS: Design and applications. *Remote Sensing and Climate Modeling: Synergies and Limitations, 7*, 5–21.

Gordon, H. R., & Morel, A. Y. (1983). Remote assessment of ocean color for interpretation of satellite visible imagery: A review. In M. Bowman (Ed.), *Lecture notes on coastal and estuarine studies, vol. 4* (pp. 1–114). New York: Springer.

Han, J. T., & Tang, D. L. (2004). Some problems in estimating a Hurst exponent—A case study of applications to climatic change. *Scientia Geographica Sinica, 24*, 177–182 (in Chinese).

Han, X. Z., Li, S. M., Luo, J. N., & Ji, X. (2008). Study on spatiotemporal change of vegetation in China since 20 years. *Arid Zone Research, 25*, 753–759 (in Chinese).

Han, G. F., Zhao, K., & Xu, J. H. (2009). Spatial-temporal change of vegetation in the Yangtze River Delta based on time series remote sensing. *Chinese Landscape Architecture, 25*, 60–64 (in Chinese).

Hong, H. S., Liu, X., Chiang, K. P., Huang, B. Q., Zhang, C. Y., Hua, J., et al. (2011). The coupling of temporal and spatial variations of chlorophyll a concentration and the East Asian monsoons in the southernTaiwan Strait. *Continental Shelf Research, 31*, S37–S47.

Huete, A., Justice, C., & Leeuwen, W. V. (1999). MODIS Vegetation index (MOD 13): Algorithm theoretical basis document, version 3. 1-133. http://modis.gsfc.nasa.gov/data/atbd/atbd_mod13.pdf

Hyde, K. J. W., O'Reilly, J. E., & Candace, A. O. (2007). Validation of SeaWiFS chlorophyll a in Massachusetts Bay. *Continental Shelf Research, 27*, 1677–1691.

Karakaya, N., & Evrendilek, F. (2011). Monitoring and validating spatio-temporal dynamics of biogeochemical properties in Mersin Bay (Turkey) using Landsat ETM. *Environmental Monitoring and Assessment, 181*, 457–464.

Kim, D., Choi, S. H., Kim, K. H., Shim, J. H., Yoo, S., & Kim, C. H. (2009). Spatial and temporal variations in nutrient and chlorophyll-a concentrations in the northern East China Sea surrounding Cheju Island. *Continental Shelf Research, 29*, 1426–1436.

Krishna, K. M. (2008). Seasonal and interannual variability of SeaWiFS-derived chlorophyll-a concentrations in waters off the southwest coast of India, 1998-2003. *Journal of Applied Remote Sensing, 2*, 023543. doi:10.1117/1.3026540.

Lasaponara, R. (2006). On the use of principal component analysis (PCA) for evaluating interannual vegetation anomalies from SPOT/VEGETATION NDVI temporal series. *Ecological Modelling, 194*, 429–434.

Morel, A., & Berthon, J. F. (1989). Surface pigments, algal biomass profiles, and potential production of the euphotic layer: Relationships reinvestigated in view of remote sensing applications. *Limnology and Oceanography, 34*, 1545–1562.

O'Reilly, J. E., Maritorena, S., Mitchell, B. G., Siegcl, D. A., Carder, K. L., Garver, S. A., et al. (1998). Ocean color chlorophyll algorithms for SeaWiFS. *Journal of Geophysical Research, 103*(11), 24,937–24,953.

Rao, A. R., & Bhattachary, D. (1999). Hypothesis testing for long-term memory in hydrologic series. *Journal of Hydrology, 216*, 183–196.

Sackmann, B., Mack, L., Logsdon, M., & Perry, M. J. (2004). Seasonal and inter-annual variability of SeaWiFS- derived chlorophyll a concentrations in waters off the Washington and Vancouver Island coasts, 1998–2002. *Deep-Sea Research Part II, 51*, 945–965.

Song, Y., & Ma, M. G. (2007). Study on vegetation cover change in northwest China based on SPOT Vegetation data. *Journal of Desert Research, 27*, 89–93 (in Chinese).

Sun, J., Wang, X., Chen, A., Ma, Y., Cui, M., & Piao, S. (2011). NDVI indicated characteristics of vegetation cover change in China's metropolises over the last three decades. *Environmental Monitoring and Assessment, 179*, 1–14.

Uz, B. M., & Yoder, J. A. (2004). High frequency and mesoscale variability in SeaWiFS chlorophyll imagery and its relation to other remotely sensed oceanographic variables. *Deep-Sea Research Part II, 51*, 1001–1017.